Geophysical Research Letters

RESEARCH LETTER
10.1029/2018GL078289

Key Points:
- A Greenland-wide heat flux map is derived from magnetic data identifying a signature related to the Iceland hotspot track
- Bouguer anomalies are consistent with thicker crust and underplating by the plume
- The heat flux map provides a new constraint for thermomechanical models of the Greenland Ice Sheet

Supporting Information:
- Supporting Information S1

Correspondence to:
Y. M. Martos,
yasmina.martos@nasa.gov

Citation:
Martos, Y. M., Jordan, T. A., Catalán, M., Jordan, T. M., Bamber, J. L., & Vaughan, D. G. (2018). Geothermal heat flux reveals the Iceland hotspot track underneath Greenland. *Geophysical Research Letters*, *45*, 8214–8222. https://doi.org/10.1029/2018GL078289

Received 10 APR 2018
Accepted 13 JUL 2018
Accepted article online 1 AUG 2018
Published online 24 AUG 2018

Geothermal Heat Flux Reveals the Iceland Hotspot Track Underneath Greenland

Yasmina M. Martos[1,2,3], Tom A. Jordan[1], Manuel Catalán[4], Thomas M. Jordan[5,6], Jonathan L. Bamber[5], and David G. Vaughan[1]

[1]British Antarctic Survey, NERC, Cambridge, UK, [2]Now at NASA Goddard Space Flight Center, Greenbelt, MD, USA, [3]Now at University of Maryland, College Park, MD, USA, [4]Royal Observatory of the Spanish Navy, Cádiz, Spain, [5]Bristol Glaciology Centre, School of Geographical Sciences, University of Bristol, Bristol, UK, [6]Department of Geophysics, Stanford University, Stanford, CA, USA

Abstract Curie depths beneath Greenland are revealed by spectral analysis of data from the World Digital Magnetic Anomaly Map 2. A thermal model of the lithosphere then provides a corresponding geothermal heat flux map. This new map exhibits significantly higher frequency but lower amplitude variation than earlier heat flux maps and provides an important boundary condition for numerical ice-sheet models and interpretation of borehole temperature profiles. In addition, it reveals new geologically significant features. Notably, we identify a prominent quasi-linear elevated geothermal heat flux anomaly running northwest–southeast across Greenland. We interpret this feature to be the relic of the passage of the Iceland hotspot from 80 to 50 Ma. The expected partial melting of the lithosphere and magmatic underplating or intrusion into the lower crust is compatible with models of observed satellite gravity data and recent seismic observations. Our geological interpretation has potentially significant implications for the geodynamic evolution of Greenland.

Plain Language Summary Heat escaping from the Earth's interior provides important clues about areas of geology and geodynamics. In addition, where a region is covered by an ice sheet, such as Greenland, variations in the heat supplied from the Earth's interior can potentially influence how the ice flows, and hence its future changes. Unfortunately, in ice covered regions direct measurements of heat flow are limited to sparse boreholes, meaning this important quantity is poorly understood. In this study we used variations in the Earth's magnetic field to map out the variations in the amount of heat being supplied to the base of the Greenland Ice Sheet from the Earth's interior. Ice sheet models incorporating these new and improved results will help better constrain future predictions of ice sheet evolution. Overall, the new map not only shows less extreme variations than previous studies, but also reveals a previously unseen band of warmer than expected rock stretching northwest to southeast across Greenland. This *band*, together with lithospheric models derived from gravity data, is interpreted to be the scar left as the Greenland tectonic plate moved over a region of hot upwelling mantle (the material beneath the tectonic plates), which now underlies Iceland.

1. Introduction

The Greenland Ice Sheet is the second largest reservoir of fresh water on Earth and ~80% of the island is ice covered. The study of the subglacial thermal conditions, geology, and lithospheric structure of the continental interior requires indirect methods, such as gravity, seismic, magnetic, and radar techniques, as rock outcrops are only accessible near the coast (Bamber, Griggs, et al., 2013; Braun et al., 2007; Fahnestock et al., 2001; Forsberg & Kenyon, 2003; Gaina et al., 2011; Levshin et al., 2016; MacGregor et al., 2016; Rogozhina et al., 2016; Steffen et al., 2017; Verhoef et al., 1996; Willis et al., 2015). Numerous regions of basal melting have been inferred from ice-penetrating radar (Bell et al., 2014; Fahnestock et al., 2001; Oswald & Gogineni, 2012) and ice borehole temperature inversion/ice flow modeling in central and northern Greenland (Buchardt & Dahl-Jensen, 2007; Dahl-Jensen et al., 2003; Grinsted & Dahl-Jensen, 2002) but the spatial relationship between these melt regions and geological boundary conditions such as geothermal heat flux is, as yet, unclear.

Greenland is mainly composed of Precambrian provinces that collided during the Early Proterozoic (Braun et al., 2007; Geological Survey of Denmark and Greenland (GEUS), 2007; Henriksen et al., 2000; Figure 1a). Comparison with other better studied continents, with similar crustal ages, suggest that regionally low geothermal heat flux is to be expected (Pollack et al., 1993; Slagstad et al., 2009). Crustal thicknesses

derived by seismology (Artemieva & Thybo, 2013; Levshin et al., 2016) and gravity data (Braun et al., 2007; Steffen et al., 2017) are consistent in showing relatively minor lateral variations, supporting the view that there has been little tectonic reworking of the continent since Early Proterozoic. An average crustal thickness between ~40 and ~36 km is suggested by seismic and gravity methods, respectively. Gravity data indicate that the thickest crust (40–50 km) is located in eastern Greenland (Braun et al., 2007; Steffen et al., 2017). Seismic studies confirm this eastern region of thick crust, but indicate an additional broad zone of thick crust (Figure 2) running approximately NNW-SSE through central Greenland (Levshin et al., 2016). Similar discrepancies have been interpreted in other areas as evidence for dense lower crust, which may be imaged more easily with seismic than gravity methods (e.g., Ferraccioli et al., 2011).

Even though Greenland is considered a stable craton, its lithosphere may have been affected by the passage of the Iceland hotspot since at least 90 Ma (Morgan, 1983). Areas of hotspot-related magmatism have been identified based on geochemical signatures both in east Greenland and on Ellesmere Island to the north (Figure 1). Potential hotspot tracks have been proposed based on regional and global tectonic reconstructions, mantle dynamic models, and rock outcrops (see Figure 3 and associated references). However, the suggested plume tracks differ significantly for times before ~60 Ma B.P. when the plume was beneath Greenland.

Forsyth et al. (1986) suggested that the Alpha Ridge and Iceland were created by the same plume, with a plume track that crosses Greenland in a NW-SE direction (Figure 1c) based on plume positions at 50 and 60 Ma (Vink, 1984) and 68 and 80 Ma (Bernero et al., 1985). This option is also compatible with the track proposed by Morgan (1983). Other authors suggest tracks trending W-E along Greenland and then north toward Ellesmere Island or north Greenland (Cox & Hart, 1986; Lawver & Müller, 1994; Müller et al., 1993; Rogozhina et al., 2016 based on Steinberger et al., 2004; O'Neill et al., 2005; Doubrovine et al., 2012).

In this paper, we present a Greenland-wide geothermal heat flux map and its associated uncertainty, derived from the World Digital Magnetic Anomaly Map 2, using spectral analyses and solving the heat conduction equation. Our new map reveals a NW-SE quasi linear region of elevated heat flux, which we interpret as the relic signature in the lithosphere beneath Greenland of the passage of the Iceland plume. Simple 2-D forward models are used to investigate the if the expected geological processes of lithospheric thinning and magmatic underplating associated with passage of a plume are consistent with satellite gravity observations.

2. Methods

2.1. Curie Depth Estimate

Magnetic anomalies are a consequence of the magnetization carried by rocks in the lithosphere (Thébault et al., 2010). These sources have ferromagnetic, ferrimagnetic, paramagnetic, or diamagnetic properties. The temperature at which the ferromagnetic minerals become paramagnetic and cannot induce a significant magnetic field is known as the Curie temperature, which is reached at the Curie depth. The Curie temperature for magnetite, the most abundant ferromagnetic mineral in the Earth's crust, is 580 °C. Here we estimated the depth to the bottom of the magnetic sources or depth of the Curie isotherm (Z_b) for Greenland using the de-fractal spectral method (Bouligand et al., 2009; Khojamli et al., 2017; Martos et al., 2017; Salem et al., 2014) with a best fit for a fractal parameter of zero, which is equivalent to use of the centroid spectral method (Li, 2011 and references therein; Salazar et al., 2017; Tanaka et al., 1999; Vargas et al., 2015). We used an analysis window size of 350 km with an overlap of 57%, see supporting information and Figures S1–S4. We applied this method to a modified version of the World Digital Magnetic Anomaly Map 2 (Catalán et al., 2016; Lesur et al., 2016). This compilation is provided as 5-km raster resolution grid and includes satellite, airborne, and shipborne data (Figure 1a), which we upward continued to a uniform altitude of 5 km above sea level on a 5-km grid.

2.2. Geothermal Heat Flux Modeling

Once we estimated the Curie depth, we built a thermal model assuming the steady-state one-dimensional heat conduction equation with radiogenic heat source (Turcotte & Schubert, 2002) to estimate the geothermal heat flux at the critical ice-bedrock interface. We considered two boundary conditions: (1) at the Curie depth, the temperature is 580 °C (Lanza & Meloni, 2006), and (2) at the ice/bedrock interface, the temperature is 0 °C (Van Liefferinge & Pattyn, 2014). The model assumed constant values of the thermal conductivity (2.8 W/mK) and radioactive heat production at the surface ($2.5{\cdot}10^{-6}$ W/m^3), such relatively

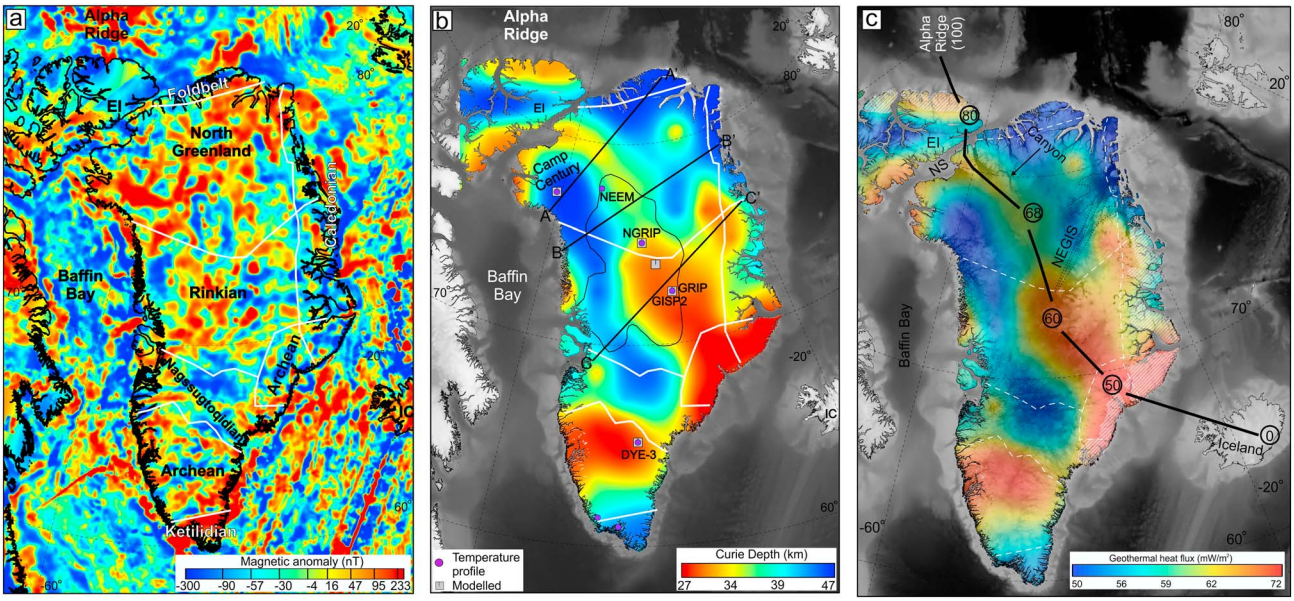

Figure 1. (a) Magnetic anomaly compilation used for determining the Curie depth. Main geological provinces are labeled. (b) Estimated Curie depth distribution. Local heat flux values are shown. Main ice cores, main geological boundaries (white lines), location of the three profiles (black solid lines) modeled using Bouguer gravity anomaly (Figure 2) and the fast body identified along the Moho by seismic tomography (thin black polygon) are displayed. (c) Geothermal heat flux map superimposed on the subglacial topography (Bamber, Griggs, et al., 2013). GEBCO relief is in the remaining background. Circles and numbers are plume track positions in millions of years based on Forsyth et al. (1986). White dashed line determines the boundary of major geological provinces. Black dashed line highlights the position of the NEGIS. Dashed shaded areas in the east coast and in EI are magma intrusions into the crust with plume origin. Black solid line is the proposed path based on this study. NEGIS = northeast Greenland ice stream; EI = Ellesmere Island; NS = Nares Strait; IC = Iceland.

low values for heat production are consistent with the known Precambrian geology of Greenland and compilations of heat production data for the formerly conjugate Fennoscandian region (Slagstad et al., 2009). The radioactive heat production of the crust is modeled as showing exponential decrease with depth with a scale depth of 8 km which is a typical value for Precambrian continental lithosphere (Artemieva & Mooney, 2001). The values for thermal conductivity and heat production were initially based on observations (Sandiford & McLaren, 2002) and were further optimized by comparing our model outputs with local heat flux estimates inferred from borehole temperature profiles in this study and by previous authors (Andersen & North Greenland Ice Core Project members, 2004; Buchardt & Dahl-Jensen, 2007; Dahl-Jensen et al., 1998, 2003; Fahnestock et al., 2001; Greve, 2005; Hansen & Langway, 1966; Petrunin et al., 2013; Sass et al., 1972; Weertman, 1968). The majority of local values were determined from the deep boreholes: GRIP, NGRIP, Camp Century, NEEM, and DYE-3, where there are ice temperature profiles available. See supporting information and Table S1 for details.

2.3. Bouguer Gravity Anomaly Calculation

Free air gravity anomalies referenced to sea level were obtained from the GOCO5s satellite derived gravity model (Mayer-Gürr and the GOCO Team, 2015). The gravity effect of onshore topography, thick ice sheet, and offshore bathymetry were calculated using the simple Bouguer slab formula, with standard densities of 2.67, 0.915, and 1.028 g/cm^3 for rock, ice, and sea water, respectively. Topography/bathymetry and ice thickness data were taken from Bamber, Griggs, et al. (2013). Detailed terrain gravity effects were not modeled as the GOCO5s field is not sensitive to such local variations. To ensure that short wavelength gravity anomalies derived from the topographic correction, but not seen in the GOCO5s gravity data, did not contaminate the final Bouguer anomaly map, we applied a 160 km low pass filter to the Bouguer correction. This filter was chosen as it matches the shortest wavelengths seen in the spectra of the GOCO5s data over Greenland. The final Bouguer gravity anomaly was calculated by subtraction of the filtered correction from the GOCO5s free air gravity anomalies.

3. Curie Depth and Geothermal Heat Flux Distributions

After applying the spectral method to the magnetic data, we obtained a map of the Curie isothermal depth at a 15-km raster resolution (Figure 1b). We estimated Curie depths as ranging from 23 to 48 km, with a mean value of 37 km, and the deepest values in the west and north of Greenland and in the interior of Ellesmere Island. As expected, shallower Curie depths characterize eastern Greenland toward the Iceland hotspot. Additionally, we calculated the uncertainty in the determination of Curie depths based on the quality of the fit of the spectral method applied (see supporting information and Figure S5). Higher uncertainties (5–6 km) are located in the Nagssugtoqidian province, while north and central Greenland present the lowest values (<3 km), as well as the east part of Ellesmere Island. The average uncertainty value is 3.5 km with a standard deviation of 1.1 km.

The heat flux map (Figure 1c) indicates values ranging from 50 to 75 mW/m^2 with an average of 60 mW/m^2. The relatively low average value for geothermal heat flux is consistent with the dominant Proterozoic/Archean age for the geology of Greenland (Geological Survey of Denmark and Greenland (GEUS), 2007; Henriksen et al., 2000), as other similar aged continents typically have low heat flux (Pollack et al., 1993). The amplitude of the variations is low. The highest values (65–75 mW/m^2) are located in the coastal part of Ellesmere Island, and in east and south Greenland, especially in the margin closest to Iceland. A well-defined zone of elevated heat flux (>200 km wide) is found crossing Greenland diagonally from the NW to the SE, separating the two main relatively low heat flux (<58 mW/m^2) areas. We also calculated, for the first time, a formal heat flux uncertainty distribution (see details in supporting information and Figure S6) for every grid point, which indicates uncertainties between 10.5 and 11 mW/m^2 with a standard deviation of 0.15 mW/m^2. These uncertainties are calculated considering a maximum range of values for the thermal parameters that play an important role in the heat equation. However, the ranges of these thermal parameters and, in turn, the uncertainties are likely much smaller given the cratonic nature of Greenland.

4. Bouguer Gravity Anomaly Map and Lithosphere Architecture

To investigate if the effects of the postulated plume on Greenland's lithosphere and the NW-SE elevated heat flux trend are reasonable, we modeled the satellite-derived Bouguer gravity anomalies across the continent (Figure 2). A main region of low values of Bouguer gravity anomalies (<−90 mGal) is identified in east and central Greenland, while the southern Archean province and the Nares Strait are also characterized by low values, consistent with regions of inferred thick crust proposed by previous seismic and gravity studies (Braun et al., 2007; Steffen et al., 2017). Three transects cutting the high heat flux trend that crosses Greenland from NW to SE were used to assess the possible impact of the plume on the lithosphere, including testing if emplacement of mafic magma at the crust/mantle interface is compatible with the observed Bouguer gravity anomalies (Figures 1b and 2).

The three gravity models (Figure 2) were performed using standard densities of 2.8, 3.3, and 3.4 g/cm^3 for the crust, lithospheric mantle, and asthenosphere, respectively (Tenzer et al., 2012; Turcotte & Schubert, 2002). Upper crustal bodies, such as sedimentary basins, are not resolved by our method due to the long wavelength of the modeled anomalies. In addition, significant sedimentary basins are not expected in the interior of Greenland given the extensive exposed basement around the ice sheet margins. Rift related sedimentary basins at the continental margins are not significant when considering processes occurring in the continental interior. Models initially assumed an isostatically defined Moho assuming a typical cratonic elastic lithosphere with an effective thickness (Te) of 60 km (Jordan & Watts, 2005; Tesauro et al., 2012; see supporting information) and a horizontal ~180 km deep lithosphere/asthenosphere boundary. These interfaces were subsequently perturbed to improve the fit to the observed data. A high-density body (3.1 g/cm^3) at the crust mantle boundary, assumed to reflect mafic magmatic underplating, was also included to test if underplating would be permissible, consistent with the observed seismic receiver function data (Levshin et al., 2016). The models show that possible thermo-mechanical erosion of the lithospheric mantle of 800–1,000 km width and 18–25 km thickness, increasing toward the southeastern profile (C-C′) would be consistent with the observed gravity data. The passage of a mantle plume beneath a continent and erosion of the lithosphere would likely generate significant volumes of magmatism. We show that a mafic body at the crust-mantle interface can account for many of the variations in the observed Bouguer anomaly along our modeled profiles. This body in the lower crust is modeled to be 8–12 km thick. The smallest volume of magmatism is modeled on Profile B-B′, where the high heat flux trend is also lowest relative to the other lines. The presence of a dense underplated body in this region

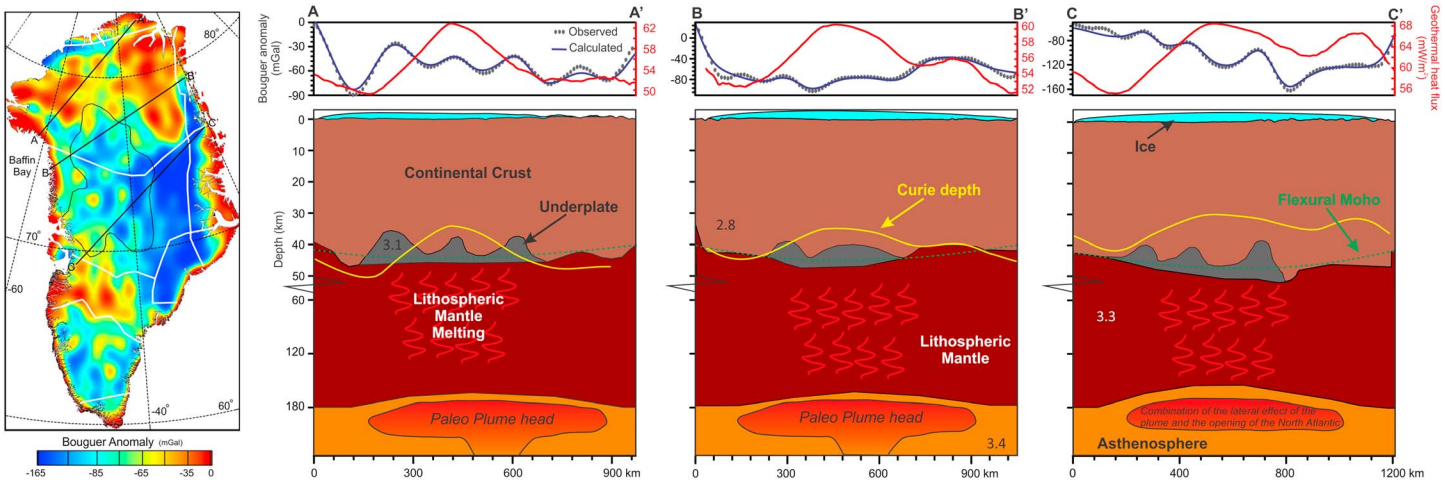

Figure 2. Left panel: Bouguer anomaly of Greenland. Black lines: profiles modeled. Thin black polygon: fast body identified along the Moho by seismic tomography. Right panel: Lithospheric architecture models using Bouguer gravity anomalies and interpretation. Densities are in grams per cubic centimeters. The estimated Curie depth is shallower than the Moho discontinuity along the high heat flux NW-SE trend. The underplate is located in the thermo-mechanically removed lithosphere and high heat flux areas due to the passage of the plume. In profile C-C′, the present effects are possibly due to the lateral contribution of the plume and the mantle dynamics related to the opening of the North Atlantic. The vertical scale is split in two different linear scales in order to see the details in the lower crust and in the lithosphere-asthenosphere boundary.

is consistent with the apparent discrepancy between ~50 km thick crust revealed by seismic data (Levshin et al., 2016) and the ~40 km thick crust indicated from regional gravity studies (Braun et al., 2007; Steffen et al., 2017), a pattern also noted and attributed to dense lower crust for example in the Gamburtsev Subglacial Mountains in Antarctica (Ferraccioli et al., 2011).

5. Discussion and Conclusions

We present a Greenland-wide geothermal heat flux distribution and, for the first time, its associated uncertainties. Low amplitude variations in the geothermal heat flux values are obtained for Greenland and Ellesmere Island. This pattern is consistent with Greenland's origin as a craton and hence, a stable continent with no major tectonic perturbations since continental amalgamation in the Early Proterozoic and low radiogenic heat production (Sass et al., 1972). Our heat flux map agrees with previous Greenland-wide studies (Fox Maule et al., 2009; Shapiro & Ritzwoller, 2004) in as far as east Greenland shows high and north Greenland shows low heat flux (see comparison in Figure S7). However, we resolve significantly higher frequency variability than previously proposed, especially in the northwest where we identify a band of high heat flux, crossing Greenland in NW-SE direction. Differences between the maps result in large measure from the higher resolution of source data we have used compared with earlier studies. Direct comparison between our method and the other two is not straightforward since ours more directly estimates the depth of the thermal discontinuity (Curie depth)—except in areas of magmatic intrusions (e.g., east Greenland) where this could represent the magnetic thickness—while others relay directly or indirectly on a mechanical discontinuity, which is then assumed to reflect a thermal boundary.

Our heat flux results are generally very close to and/or within the uncertainty of previously inferred local values (Andersen & North Greenland Ice Core Project members 2004; Buchardt & Dahl-Jensen, 2007; Dahl-Jensen et al., 1998, 2003; Greve, 2005; Hansen & Langway, 1966; Petrunin et al., 2013; Sass et al., 1972; Weertman, 1968; see supporting information and Table S1). Local values at the NEEM, Camp Century and GRIP boreholes (58, 41–50, and 51–60 mW/m^2, respectively) are all consistent with the values and uncertainty range of our heat map, whilst the local values at DYE-3 (20–25 mW/m^2) are significantly less than our predictions. However, since the DYE-3 temperature profile is far from steady-state (Dahl-Jensen et al., 1998), the local heat flux estimates at DYE-3 are likely to be less accurate than the other cores. Since the basal temperature at NGRIP is above pressure melting point, local heat flux estimates are less well constrained than other boreholes, and range from 55 to 160 mW/m^2 (encompassing our value of 63 mW/m^2). An area of anomalously high heat flux (970 mW/m^2) inferred by Fahnestock et al. (2001)

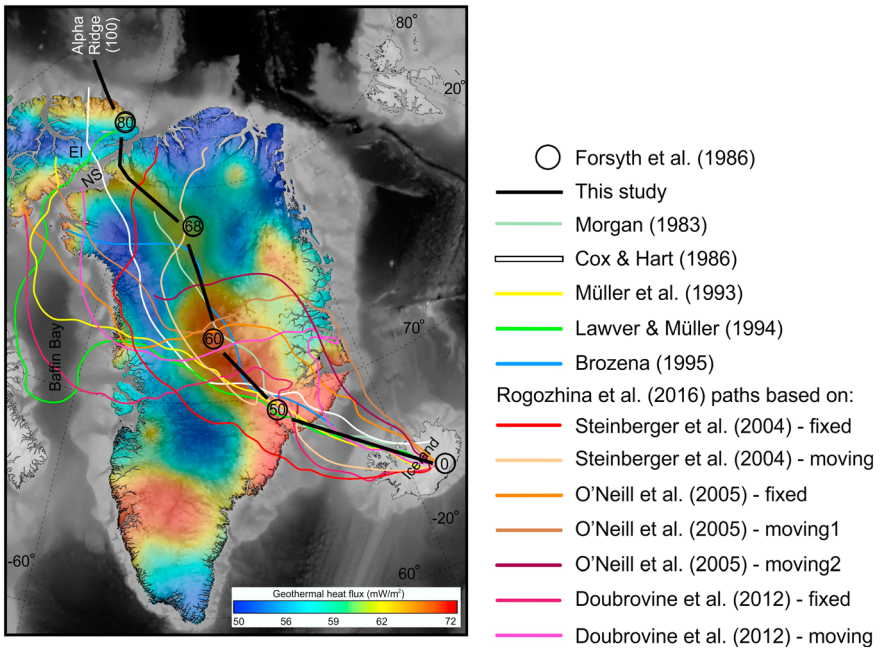

Figure 3. New heat flux distribution for Greenland and main Iceland hotspot tracks proposed since the 80s. Circles and numbers are plume track positions in millions of years based on Forsyth et al. (1986). Fixed: considering Iceland hotspot fixed. Moving: considering Iceland hotspot moving. EI = Ellesmere Island; NS = Nares Strait.

from ice-penetrating radiostratigraphy in central Greenland is likely to be a localized anomaly limited to a horizontal extent of $<$10 km. Such an anomaly, if it exists, would not be resolved by our technique. However, we do identify an area of enhanced heat flux ($>$65 mW/m^2) in the same region, which is consistent with the previous hypothesis that geothermal heat exerts a strong influence on ice flow in the ice sheet interior (Fahnestock et al., 2001). Finally, considering the differences between local values and proposed models (Fox Maule et al., 2009; Shapiro & Ritzwoller, 2004, our study), we obtain almost a 50% higher internal coherency than previous models (see supporting information).

Our new geothermal heat flux map is valuable for several areas of glaciological research, including ice-sheet modeling, ice-core site selection, and subglacial hydrology. The ice-sheet modeling study by Rogozhina et al. (2012) established that an assumption of spatially uniform heat flux produces an overall better fit to observational data than parametrizing using either the maps of Shapiro and Ritzwoller (2004) or Fox Maule et al. (2009). Since the overall amplitude variation of our map is much lower than these previous maps, we believe the new map provides an important thermal boundary condition for ice-sheet models and will improve the spatial distribution of predicted thawed bed in these models. Our new heat flux map and its uncertainties will help to constrain estimates of basal temperature and the basal thermal state, which in turn, will help to provide more realistic models of ice dynamics and improve the knowledge of subglacial hydrology distribution across Greenland. For example, the 750-km long deep canyon that extends from central Greenland to the northwest (Bamber, Siegert, et al., 2013) coincides with the NW-SE quasi-linear region of high heat flux in Figure 1c. The elevated heat flux in this region, particularly in central Greenland, potentially facilitates production of subglacial water which could be linked to the size and extent of the canyon. While it is believed that the canyon predates the ice sheet (Bamber, Siegert, et al., 2013), it was also noted that it provides a route for subglacial water, which would act to enhance rates of erosion when the ice sheet is present (Drewry, 1986). The presence of a thawed bed in the canyon region is supported by the ice-penetrating radar studies of Oswald and Gogineni (2012; bed-echo data) and Bell et al. (2014; radio-stratigraphy)—refer to Rogozhina et al. (2016) for a data compilation map. However, Greenland water predictions using bed-echo data can be ambiguous (Jordan et al., 2017), and assessing the influence of the elevated heat flux on the thermal state will likely require the development of refined radar analysis techniques. Additionally, inferences from thermomechanical models, ice velocity and surface properties, suggest that some of this region is below pressure melting point (MacGregor et al., 2016), and thus water may not route down the present-day canyon.

The variation of geothermal heat flux shows agreement with some of the inferred geological provinces and boundaries predicted beneath the ice sheet (Figure 1c). The southernmost and east coast Archean provinces correlate with generally elevated heat flux. However, there is not a clear correlation between heat flux values and the proposed Nagssugtoqidian, Rinkian, and north Greenland geological provinces within the center of the continent. This means that the heat flux signatures we see in the continental interior are not easily explained by the known geology. Other authors have suggested that geothermal heat flux anomalies may reflect the passage of the Iceland Plume (Rogozhina et al., 2016). We suggest that the quasi-linear elevated heat flux feature which crosscuts both the Rinkian and north Greenland blocks reflects the path of the Iceland hotspot beneath the continent. Although nonunique, models of the long wavelength Bouguer gravity anomaly in this region show that thinning of the lithosphere and significant underplating by dense mafic material, as expected in the case of the passage of a mantle plume, would both be permissible. The presence of a dense underplated body approximately aligned with the heat flow anomaly is in agreement with the most recent seismic tomographic study (Levshin et al., 2016), which show an elongated high shear wave velocity (likely high density) zone in central Greenland above the Moho (Figure 1b). Our conceptual model is that the plume thermo-mechanically removed part of the lithospheric mantle (Figure 2). This would have been associated with partial melting of the lithosphere and production of magma, which was underplated and intruded into the lower crust. Such a high density body at the base of the crust is consistent with the process of underplating observed elsewhere (Thybo & Artemieva, 2013). For example, a similar process may have occurred in central India, a region strongly affected by the activity of Reunion mantle plume, where more than 12 km of mafic material was accreted into the lower crust (Reddy & Rao, 2013).

Simultaneously to the underplating process in Greenland, the plume head would have heated the lithosphere by conduction, locally moving isotherms to shallower depths. Addition and concentration of radiogenic material due to partial melting of the lithosphere may have acted to further enhance the long-term heat flux along the plume track. Together, these processes can explain the elevated heat flux and the shallower Curie depths along the plume track (Figures 1b, 1c, and 2). Long-term cooling of the lithosphere after the passage of the plume may explain why the NW-SE elevated heat flux trend is subdued in the north Greenland province. The Curie depth profile along this trend shows a clear cooling effect such the one observed in the oceans and in other age progressive magmatic provinces (Brott et al., 1981; see Figure S8).

The precise plume track pre-65 Ma under Greenland is still under debate. Although there is little direct evidence for its existence, many authors have linked Cretaceous magmatism in the High Arctic to the plume track. Specifically, Forsyth et al. (1986) propose that the Alpha Ridge and Iceland were created by the same plume, based on their integration and study of seismic refraction, magnetic anomalies, and other geophysical and geological information.

Many other possible plume tracks have been proposed beneath Greenland, but while all agree that east Greenland was affected by the Iceland plume ~60 Ma B.P., the earlier plume track is contested (Figure 3). Our geothermal heat flux distribution as well as our gravity modeling and seismic tomography (Artemieva & Thybo, 2013; Levshin et al., 2016) are consistent with a plume track that crossed Greenland from NW to SE (Figures 1c and 3). This path agrees with the one proposed by Forsyth et al. (1986) and Morgan (1983). Based on our work, integrating geothermal heat flux derived by aeromagnetic data, gravity modeling, seismic tomography, geology, and plume track reconstructions, we conclude that the NW-SE elevated heat flux trend is the relic of the thermal effects of the plume track. In this scenario the high heat flux is produced by the remnant of the plume passage, which deformed the isotherms, and with possible additional radiogenic heat production by the materials attached to the lower crust during the underplating process. We found no geophysical or geological evidence for a plume track with a W-E orientation or a track closer to the west coast or Baffin Bay. However, we acknowledge the possible lateral effects of the plume in the lithosphere being responsible for the opening of Baffin Bay and associated magmatism in western Greenland. In east Greenland, we see the most elevated heat flux, which is probably related to a combination of the lateral effect of the plume and the mantle processes associated with the opening of the North Atlantic.

Acknowledgments
We wish to thank three anonymous reviewers for their constructive comments and suggestions who helped us to improve our manuscript. Y. M. M. thanks the Marie Skłodowska-Curie Program (European Commission Grant ID 657187) for supporting this research. The supporting information file contains details about the magnetic and borehole data, methodology, and results. The resulting Curie depth and geothermal heat flux model as well as their associated uncertainties can be found at PANGAEA (https://doi.pangaea.de/10.1594/PANGAEA.892973).

References

Andersen, K. K., & North Greenland Ice Core Project members (2004). High-resolution record of Northern Hemisphere climate extending into the last interglacial period. *Nature*, *431*(7005), 147–151.

Artemieva, I. M., & Mooney, W. D. (2001). Thermal thickness and evolution of Precambrian lithosphere: A global study. *Journal of Geophysical Research*, *106*(B8), 16,387–16,414. https://doi.org/10.1029/2000JB900439
Artemieva, I. M., & Thybo, H. (2013). EUNAseis: A seismic model for Moho and crustal structure in Europe, Greenland, and the North Atlantic region. *Tectonophysics*, *609*, 97–153. https://doi.org/10.1016/j.tecto.2013.08.004
Bamber, J. L., Griggs, J. A., Hurkmans, R. T. W. L., Dowdeswell, J. A., Gogineni, S., Howat, I., et al. (2013). A new bed elevation dataset for Greenland. *The Cryosphere*, *7*(2), 499–510. https://doi.org/10.5194/tc-7-499-2013
Bamber, J. L., Siegert, M. J., Griggs, J. A., Marshall, S. J., & Spada, G. (2013). Paleofluvial mega-canyon beneath the central Greenland ice sheet. *Science*, *341*(6149), 997–999. https://doi.org/10.1126/science.1239794
Bell, R. E., Tinto, K., Das, I., Wolovick, M., Chu, W., Creyts, T. T., et al. (2014). Deformation, warming and softening of Greenland's ice by refreezing meltwater. *Nature Geoscience*, *7*(7), 497–502. https://doi.org/10.1038/ngeo2179
Bernero, C., Kovacs, L. C., Vogt, P. R., & Pilger, R. H. Jr. (1985). *Paleobathymetry and plate reconstructions, in Residual magnetic anomaly chart of the Arctic Ocean region: Geological society of America map and chart series MC-53*.
Bouligand, C., Glen, J. M. G., & Blakely, R. J. (2009). Mapping curie temperature depth in the western United States with a fractal model for crustal magnetisation. *Journal of Geophysical Research*, *114*, B11104. https://doi.org/10.1029/2009JB006494
Braun, A., Kim, H. R., Csatho, B., & von Frese, R. R. (2007). Gravity-inferred crustal thickness of Greenland. *Earth and Planetary Science Letters*, *262*(1-2), 138–158. https://doi.org/10.1016/j.epsl.2007.07.050
Brott, C. A., Blackwell, D. D., & Ziagos, J. P. (1981). Thermal and tectonic implications of heat flow in the eastern Snake River Plain, Idaho. *Journal of Geophysical Research*, *86*(B12), 11,709–11,734. https://doi.org/10.1029/JB086iB12p11709
Buchardt, S. L., & Dahl-Jensen, D. (2007). Estimating the basal melt rate at NorthGRIP using a Monte Carlo technique. *Annals of Glaciology*, *45*(1), 137–142. https://doi.org/10.3189/172756407782282435
Catalán, M., Dyment, J., Choi, Y., Hamoudi, M., Lesur, V., Thebault, E., et al. (2016). Making a better magnetic map. *Eos*, *97*. https://doi.org/10.1029/2016EO054645
Cox, A., & Hart, R. B. (1986). *Plate tectonics: How it works*. Oxford, UK: Blackwell Scientific Publications.
Dahl-Jensen, D., Gundestrup, N., Gogineni, S. P., & Miller, H. (2003). Basal melt at NorthGRIP modeled from borehole, ice-core and radio-echo sounder observations. *Annals of Glaciology*, *37*(1), 207–212. https://doi.org/10.3189/172756403781815492
Dahl-Jensen, D., Mosegaard, K., Gundestrup, N., Clow, G. D., Johnsen, S. J., Hansen, A. W., & Balling, N. (1998). Past temperatures directly from the Greenland ice sheet. *Science*, *282*(5387), 268–271. https://doi.org/10.1126/science.282.5387.268
Doubrovine, P. V., Steinberger, B., & Torsvik, T. H. (2012). Absolute plate motions in a reference frame defined by moving hotspots in the Pacific, Atlantic and Indian oceans. *Journal of Geophysical Ressearch*, *117*, B09101. https://doi.org/10.1029/2011JB009072
Drewry, D. J. (1986). *Glacial geologic processes* (p. 276). London: Edward Arnold.
Fahnestock, M., Abdalati, W., Joughin, I., Brozena, J., & Gogineni, P. (2001). High geothermal heat flow, basal melt, and the origin of rapid ice flow in central Greenland. *Science*, *294*(5550), 2338–2342. https://doi.org/10.1126/science.1065370
Ferraccioli, F., Finn, C. A., Jordan, T. A., Bell, R. E., Anderson, L. M., & Damaske, D. (2011). East Antarctic rifting triggers uplift of the Gamburtsev Mountains. *Nature*, *479*(7373), 388–392. https://doi.org/10.1038/nature10566
Forsberg, R., & Kenyon, S. (2003). The Arctic Gravity Project. http://www.nima.mil/GandG/agp/
Forsyth, D. A., Morel-a-l'Huissier, P., Asudeh, I., & Green, A. G. (1986). Alpha ridge and Iceland-products of the same plume? *Journal of Geodynamics*, *6*(1–4), 197–214. https://doi.org/10.1016/0264-3707(86)90039-6
Fox Maule, C., Purucker, M. E., & Olsen, N. (2009). Inferring magnetic crustal thickness and geothermal heat flux from crustal magnetic field models, estimating the geothermal heat flux beneath the Greenland ice sheet. *Danish Climate Centre Report*, *9*(09).
Gaina, C., Werner, S., Saltus, R., Maus, S., & the CAMP-GM group (2011). Circum-Arctic mapping project: New magnetic and gravity anomaly maps of the Arctic. In A. M. Spencer, A. F. Embry, D. L. Gautier, A. V. Stoupakova, & K. Sørensen (Eds.), *Arctic petroleum geology* (Vol. 35, pp. 39–48). London, Memoirs: Geological Society.
Geological Survey of Denmark and Greenland (GEUS) (2007). Geological Map of Greenland. Retrieved from http://www.geus.dk/geuspage-uk.htm
Greve, R. (2005). Relation of measured basal temperatures and the spatial distribution of the geothermal heat flux for the Greenland ice sheet. *Annals of Glaciology*, *42*(1), 424–432. https://doi.org/10.3189/172756405781812510
Grinsted, A., & Dahl-Jensen, D. (2002). A Monte Carlo-tuned model of the flow in the NorthGRIP area. *Annals of Glaciology*, *35*, 527–530. https://doi.org/10.3189/172756402781817130
Hansen, B. L., & Langway, C. C. Jr. (1966). Deep core drilling in ice and core analysis at Camp Century, Greenland, 1961-1966. *Antarctic Journal of the United States*, *1*(5), 207–208.
Henriksen, N., Higgins, A. K., Kalsbeek, F., & Pulvertaft, T. C. R. (2000). Greenland from Archaean to quaternary, descriptive text to the geological map of Greenland 1: 2,500,000. *Geology of Greenland Survey Bulletin*, *185*, 93.
Jordan, T. A., & Watts, A. B. (2005). Gravity anomalies, flexure and the elastic thickness structure of the India–Eurasia collisional system. *Earth and Planetary Science Letters*, *236*(3-4), 732–750. https://doi.org/10.1016/j.epsl.2005.05.036
Jordan, T. M., Cooper, M. A., Schroeder, D. M., Williams, C. N., Paden, J. D., Siegert, M. J., & Bamber, J. L. (2017). Self-affine subglacial roughness: Consequences for radar scattering and basal water discrimination in northern Greenland. *The Cryosphere*, *11*(3), 1247–1264. https://doi.org/10.5194/tc-11-1247-2017
Khojamli, A., Ardejani, F. D., Moradzadeh, A., Kalate, A. N., Kahoo, A. R., & Porkhial, S. (2017). Determining fractal parameter and depth of magnetic sources for Ardabil geothermal area using aeromagnetic data by de-fractal approach. *Journal of Mining and Environment*, *8*(1), 93–101.
Lanza, R., & Meloni, A. (2006). *The Earth's Magnetism*. Berlin: Springer-Verlag.
Lawver, L. A., & Müller, R. D. (1994). Iceland hotspot track. *Geology*, *22*(4), 311–314. https://doi.org/10.1130/0091-7613(1994)022<0311:IHT>2.3.CO;2
Lesur, V., Hamoudi, M., Choi, Y., Dyment, J., & Thébault, E. (2016). Building the second version of the world digital magnetic anomaly map (WDMAM). *Earth, Planets and Space*, *68*, 1–13.
Levshin, A., Shen, W., Barmin, M., & Ritzwoller, M. (2016). Surface-wave studies of the Greenland crustal structure using ambient seismic noise, 35th General Assembly of European Seismological Commission.
Li, C.-F. (2011). An integrated geodynamic model of the Nankai subduction zone and neighboring regions from geophysical inversion and modeling. *Journal of Geodynamics*, *51*(1), 64–80. https://doi.org/10.1016/j.jog.2010.08.003
MacGregor, J. A., Fahnestock, M. A., Catania, G. A., Aschwanden, A., Clow, G. D., Colgan, W. T., et al. (2016). A synthesis of the basal thermal state of the Greenland ice sheet. *Journal of Geophysical Research: Earth Surface*, *121*, 1328–1350. https://doi.org/10.1002/2015JF003803
Martos, Y. M., Catalán, M., Jordan, T. A., Golynsky, A., Golynsky, D., Eagles, G., & Vaughan, D. G. (2017). Heat flux distribution of Antarctica unveiled. *Geophysical Research Letters*, *44*, 11,417–11,426. https://doi.org/10.1002/2017GL075609

Mayer-Gürr, T., & the GOCO Team (2015). The combined satellite gravity field model GOCO05S. Geophysical research abstracts, Vol. 17, EGU2015-12364, EGU general assembly, Vienna.
Morgan, W. J. (1983). Hotspot tracks and the early rifting of the Atlantic. *Tectonophysics*, *94*(1–4), 123–139. https://doi.org/10.1016/0040-1951(83)90013-6
Müller, R. D., Royer, J. Y., & Lawver, L. A. (1993). Revised plate motions relative to the hotspots from combined Atlantic and Indian Ocean hotspot tracks. *Geology*, *21*(3), 275–278. https://doi.org/10.1130/0091-7613(1993)021<0275:RPMRTT>2.3.CO;2
O'Neill, C., Müller, R. D., & Steinberger, B. (2005). On the uncertainties in hotspot reconstructions, and the significance of moving hotspot reference frames. *Geochemistry, Geophysics, Geosystems*, *6*, Q04003. https://doi.org/10.1029/2004GC000784
Oswald, G. K. A., & Gogineni, S. P. (2012). Mapping basal melt under the northern Greenland ice sheet. IEEE Trans. *Geoscience Remote Sensing*, *50*(2), 585–592. https://doi.org/10.1109/TGRS.2011.2162072
Petrunin, A. G., Rogozhina, I., Vaughan, A. P. M., Kukkonen, I. T., Kaban, M. K., Koulakov, I., & Thomas, M. (2013). Heat flux variations beneath central Greenland's ice due to anomalously thin lithosphere. *Nature Geoscience*, *6*(9), 746–750. https://doi.org/10.1038/ngeo1898
Pollack, H. N., Hurter, S. J., & Johnson, J. R. (1993). Heat flow from the Earth's interior: Analysis of the global data set. *Reviews of Geophysics*, *31*(3), 267–280. https://doi.org/10.1029/93RG01249
Reddy, P. R., & Rao, V. V. (2013). Seismic images of the continental Moho of the Indian shield. *Tectonophysics*, *609*, 217–233. https://doi.org/10.1016/j.tecto.2012.11.022
Rogozhina, I., Hagedoorn, J. M., Martinec, Z., Fleming, K., Soucek, O., Greve, R., & Thomas, M. (2012). Effects of uncertainties in the geothermal heat flux distribution on the Greenland ice sheet: An assessment of existing heat flow models. *Journal of Geophysical Research*, *117*, F02025. https://doi.org/10.1029/2011JF002098
Rogozhina, I., Petrunin, A. G., Vaughan, A. P., Steinberger, B., Johnson, J. V., Kaban, M. K., et al. (2016). Melting at the base of the Greenland ice sheet explained by Iceland hotspot history. *Nature Geoscience*, *9*(5), 366–369. https://doi.org/10.1038/ngeo2689
Salazar, J. M., Vargas, C. A., & Leon, H. (2017). Curie point depth in the SW Caribbean using the radially averaged spectra of magnetic anomalies. *Tectonophysics*, *694*, 400–413. https://doi.org/10.1016/j.tecto.2016.11.023
Salem, A., Green, C., Ravat, D., Singh, K. H., East, P., Fairhead, J. D., et al. (2014). Depth to Curie temperature across the central Red Sea from magnetic data using the de-fractal method. *Tectonophysics*, *624-625*, 75–86. https://doi.org/10.1016/j.tecto.2014.04.027
Sandiford, M., & McLaren, S. (2002). Tectonic feedback and the ordering of heat producing elements within the continental lithosphere. *Earth and Planetary Science Letters*, *204*(1-2), 133–150. https://doi.org/10.1016/S0012-821X(02)00958-5
Sass, J. H., Nielsen, B. L., Wollenberg, H. A., & Munroe, R. J. (1972). Heat flow and surface radioactivity at two sites in South Greenland. *Journal of Geophysical Research*, *77*(32), 6435–6444. https://doi.org/10.1029/JB077i032p06435
Shapiro, N. M., & Ritzwoller, M. H. (2004). Inferring surface heat flux distributions guided by a global seismic model: Particular application to Antarctica. *Earth and Planetary Science Letters*, *223*(1-2), 213–224. https://doi.org/10.1016/j.epsl.2004.04.011
Slagstad, T., Balling, N., Elvebakk, H., Midttømme, K., Olesen, O., Olsen, L., & Pascal, C. (2009). Heat-flow measurements in late Palaeoproterozoic to Permian geological provinces in south and central Norway and a new heat-flow map of Fennoscandia and the Norwegian–Greenland Sea. *Tectonophysics*, *473*(3-4), 341–361. https://doi.org/10.1016/j.tecto.2009.03.007
Steffen, R., Strykowski, G., & Lund, B. (2017). High-resolution Moho model for Greenland from EIGEN-6C4 gravity data. *Tectonophysics*, *706*, 206–220.
Steinberger, B., Sutherland, R., & O'Connell, R. J. (2004). Prediction of Emperor-Hawaii seamount locations from a revised model of plate motion and mantle flow. *Nature*, *430*(6996), 167–173. https://doi.org/10.1038/nature02660
Tanaka, A., Okubo, Y., & Matsubayashi, O. (1999). Curie point depth based on spectrum analysis of the magnetic anomaly data in East and Southeast Asia. *Tectonophysics*, *306*(3-4), 461–470. https://doi.org/10.1016/S0040-1951(99)00072-4
Tenzer, R., Novák, P., Gladkikh, V., & Vajda, P. (2012). Global crust-mantle density contrast estimated from EGM2008, DTM2008, CRUST2. 0, and ICE-5G. *Pure and Applied Geophysics*, *169*(9), 1663–1678. https://doi.org/10.1007/s00024-011-0410-3
Tesauro, M., Audet, P., Kaban, M. K., Bürgmann, R., & Cloetingh, S. (2012). The effective elastic thickness of the continental lithosphere: Comparison between rheological and inverse approaches. *Geochemistry, Geophysics, Geosystems*, *13*, Q09001. https://doi.org/10.1029/2012GC004162
Thébault, E., Purucker, M., Whaler, K. A., Langlais, B., & Sabaka, T. J. (2010). The magnetic field of the Earth's lithosphere. *Space Science Reviews*, *155*(1–4), 95–127. https://doi.org/10.1007/s11214-010-9667-6
Thybo, H., & Artemieva, I. M. (2013). Moho and magmatic underplating in continental lithosphere. *Tectonophysics*, *609*, 605–619. https://doi.org/10.1016/j.tecto.2013.05.032
Turcotte, D. L., & Schubert, G. (2002). *Geodynamics* (Vol. 2014, p. 456). Cambridge: Cambridge University Press.
Van Liefferinge, B., & Pattyn, F. (2014). Basal temperature calculations of the Greenland ice sheet. Abstract and poster retrieved from the International Symposium on Glaciers and Ice Sheets Contribution to Sea-Level Change (Observations, Modelling and Prediction). Chamonix-Mont-Blanc, France, 26–30 May 2014.
Vargas, C. A., Idarraga-Garcia, J., & Salazar, J. M. (2015). Curie point depths in northwestern South America and the southwestern Caribbean Sea. In C. Bartolini & P. Mann (Eds.), *Petroleum geology and potential of the Colombian Caribbean margin* (Vol. 108, pp. 179–200). Tulsa, OK: AAPG Memoir. https://doi.org/10.1306/13531936M1083642
Verhoef, J., Roest, W. R., Macnab, R., Arkani-Hamed, J., & members of the project team (1996). Magnetic anomalies of the Arctic and Atlantic Oceans and adjacent land areas. GSC Open File Rep. 3125, Geological Survey of Canada, Ottawa, 225 pp.
Vink, G. E. (1984). A hotspot model for Iceland and the Voring Plateau. *Journal of Geophysical Research*, *89*(B12), 9949–9959. https://doi.org/10.1029/JB089iB12p09949
Weertman, J. (1968). Comparison between measured and theoretical temperature profiles of the Camp Century, Greenland, borehole. *Journal of Geophysical Research*, *73*(8), 2691–2700. https://doi.org/10.1029/JB073i008p02691
Willis, M. J., Herried, B. G., Bevis, M. G., & Bell, R. E. (2015). Recharge of a subglacial lake by surface meltwater in northeast Greenland. *Nature*, *518*(7538), 223–227. https://doi.org/10.1038/nature14116